

Probing the strange Higgs coupling at e^+e^- colliders using light-jet flavor tagging

J. Duarte-Campderros,^{1,2,*} G. Perez,^{3,†} M. Schlaffer,^{3,‡} and A. Soffer^{4,§}

¹*Universidad de Cantabria Instituto de Fisica de Cantabria (IFCA) Avda. Los Castros s/n, E-39005 Santander, Spain*

²*European Organization for Nuclear Research (CERN) EP-CMX Dept. CH-1211 Geneva 23, Switzerland*

³*Department of Particle Physics and Astrophysics,*

Weizmann Institute of Science, Rehovot 7610001, Israel

⁴*School of Physics and Astronomy, Tel-Aviv University, Tel-Aviv 69978, Israel*

We propose a method to probe the coupling of the Higgs to strange quarks by tagging strange jets at future lepton colliders. For this purpose we describe a jet-flavor observable, J_F , that is correlated with the flavor of the quark associated with the hard part of the jet. Using this variable, we set up a strangeness tagger aimed at studying the decay $h \rightarrow s\bar{s}$. We determine the sensitivity of our method to the strange Yukawa coupling, and find it to be of the order of the standard-model expectation.

The hierarchical structure of the masses and mixing angles of the fundamental, point-like matter fields is one of the unsolved mysteries of the standard model (SM) of elementary particles. This *flavor puzzle* extends beyond the SM, since new-physics models are severely constrained by measurements of flavor observables. Within the SM, the flavor structure is trivially encoded by the structure of the Yukawa interactions: the Yukawa coupling of fermion f to the physical Higgs is given by the ratio of the fermion mass to the Higgs vacuum expectation value, $y_f = m_f/v$. Beyond the SM, various alternatives motivated by the flavor puzzle predict significant deviations from this structure (see, *e.g.*, Refs. [1–6]). Now that we have entered the era of precision Higgs measurements, one can begin to tackle this question experimentally, opening a new direction in flavor physics.

Experimental tests of the Yukawa interactions are performed in terms of the signal strength μ_P , defined as the ratio of the measured production cross section or branching ratio of the process P to the SM expectation for this quantity. The latest results from the ATLAS [7–9] collaboration are

$$\mu_{tth} = 1.32_{-0.26}^{+0.28}, \quad \mu_{bb} = 1.01_{-0.20}^{+0.20}, \quad \mu_{\tau\tau} = 1.09_{-0.30}^{+0.35}, \quad (1)$$

where $P = tth$ refers to the process $pp \rightarrow t\bar{t}h$ and $P = bb$ denotes the decay $h \rightarrow b\bar{b}$, etc. Similarly, the CMS [10] collaboration has measured

$$\mu_{tth} = 1.18_{-0.27}^{+0.30}, \quad \mu_{bb} = 1.12_{-0.29}^{+0.29}, \quad \mu_{\tau\tau} = 1.02_{-0.24}^{+0.26}. \quad (2)$$

Within the large uncertainties, these results are in good agreement with the SM expectation for the third-generation fermions, for which the Yukawa couplings are large and thus easier to measure. Precision will improve as the experiments collect more data.

However, it is important to note that the flavor puzzle is related to the mass hierarchy among all three generations of up-type quarks (u, c, t), down-type quarks ($d, s,$

b) and charged leptons (e, μ, τ). Therefore, direct measurements of the smaller couplings of the Higgs to the first two generations of the different sectors are also necessary. So far, only upper bounds on the corresponding signal strengths have been obtained [11–14],

$$\begin{aligned} \mu_{\mu\mu} &\lesssim 2.8, & \mu_{ee} &\lesssim 3.7 \times 10^5, \\ \mu_{cc} &\lesssim 110, & \mu_{ss} &\lesssim 7.2 \times 10^8. \end{aligned} \quad (3)$$

There is a clear path towards measuring the Yukawa couplings of the muon [11], charm quark [15], and possibly even the electron [16]. For the light quarks, the situation is much less clear. It is possible that their Yukawa couplings could be probed exclusively [3] or indirectly [17–21]. However, these methods are characterized by small rates and/or are subject to large QCD backgrounds that are difficult to control (see, *e.g.*, Refs. [22, 23]).

In this letter we propose using a strangeness tagger, inspired by $Z \rightarrow s\bar{s}$ measurements at the DELPHI [24] and SLD [25] experiments, for probing the Higgs coupling to the strange quark via the $h \rightarrow s\bar{s}$ decay. We first present the basic idea and describe a new jet-flavor variable, J_F , for determining the light flavor of a jet or other collection of particles. Subsequently, we implement J_F for strange jets and combine it with a simple method for rejecting background from heavy-flavor jets. This combination of a cut on J_F and the heavy-flavor rejection as well as a choice for the parameter intended to select kaons is denoted as s -tagger in the following. Finally, we apply this s -tagger to a collider scenario with background from other Higgs decays and non-Higgs events.

Since the branching ratio for $h \rightarrow s\bar{s}$ is small, the measurement requires a large number of Higgs bosons in a very clean environment. Therefore, we limit the discussion to lepton colliders, having in mind the International Linear Collider (ILC) [26], the Future Circular Collider in electron mode (FCC-ee) [27], and the Circular Electron Positron Collider (CEPC) [28]. These proposed colliders would run at a center-of-mass energy $\sqrt{s} = 250$ GeV, where the cross section for associated Higgs production, $e^+e^- \rightarrow Zh$, peaks at $\sigma \approx 210$ fb for unpolarized beams [29, 30]. We therefore adopt this scenario for this letter.

* jorge.duarte.campderros@cern.ch

† gilad.perez@weizmann.ac.il

‡ matthias.schlaffer@weizmann.ac.il

§ asoffer@post.tau.ac.il

Flavor tagging relies on the idea that the flavor of a parton that belongs to the hard part of the event is correlated with properties of the collection of final-state hadrons originating from that parton. This collection may be the hadrons in a jet or any other part of the event, *e.g.*, a hemisphere defined by a particular axis. We use the term *jet* as a generic umbrella term for both, with *jet flavor* referring to the flavor of the primary parton that gave rise to the jet. The process of determining jet flavor is referred to as *flavor tagging*.

While QCD conserves flavor, it does impact the particle composition of a jet, thus affecting jet flavor tagging. For example, flavor-blind gluon splitting can result in a quark appearing inside the jet while its partner antiquark does not, resulting in the creation of flavor that is differential in phase space [31]. In the case of heavy quarks, this can be mitigated perturbatively by modifying the clustering algorithm used to construct the jet. This is done either by undoing the flavor creation by gluon splitting [31] or by allowing the jet to form a higher representation (beyond fundamental) of the SM global flavor group [32]. Here, we attempt to tackle the same issue for the light-flavor quarks. The price to pay is that we must give up some perturbative control and hence calculability. Specifically, the jet-flavor variable that we define below is safe against soft but not collinear radiation.

While the processes of showering and hadronization degrade the flavor-tagging capability, some of the correlation between the primary parton and the final-state hadrons remains. To exploit this, we define a new jet-flavor variable,

$$J_F = \frac{\sum_H \mathbf{p}_H \cdot \hat{\mathbf{s}} R_H}{\sum_H \mathbf{p}_H \cdot \hat{\mathbf{s}}}. \quad (4)$$

Here, the sum is over all hadrons inside the jet, \mathbf{p}_H is the momentum vector of the hadron H , R_H is its quantum number or numbers in the flavor representation of interest, and $\hat{\mathbf{s}}$ is the normalized jet axis. In our case of a Higgs boson produced approximately at rest and undergoing a $h \rightarrow jj$ decay, $|\sum_H \mathbf{p}_H| \approx m_h/2$, so that the denominator is nonzero, and J_F is well defined. Here and in the following we use $h \rightarrow jj$ to denote a Higgs decay into a final state of two gluons or a quark-anti-quark pair.

As our focus is on strangeness tagging, we use only the SU(3) flavor composition for evaluating R_H . For further simplicity, we consider only pions and kaons, which constitute the majority of final-state hadrons. Since $m_{u,d} \ll m_s \sim \Lambda_{\text{QCD}}$, the SU(3) flavor symmetry is broken in a rather strong way by the strange-quark mass. Therefore, it is enough to consider only strangeness, assigning $R_{K^\pm} = \mp 1$ and $R_{\pi^\pm,0} = 0$. The opposite sign of R_{K^\pm} for oppositely charged kaons ensures that kaons originating from $g \rightarrow s\bar{s}$ contribute minimally to J_F . The presence of neutral kaons weakens the ability to perform strangeness tagging for two reasons. First, it is impossible to determine whether a neutral kaon has strangeness

1 or -1 . Second, only the K_S decays in a clearly distinguishable manner, while the K_L gives rise to calorimeter energy deposits that are not unique. Therefore, a reasonable, minimal-bias approach is to assign $R_{K_S} = 1$ or -1 to each K_S in the jet, choosing the set of values that minimizes the value of $|J_F|$.

We test our s -tagger on $e^+e^- \rightarrow Zh$ events that are generated at $\sqrt{s} = 250$ GeV and showered using PYTHIA version 8.219 [33, 34]. For the purpose of studying background from hadronic W decays, we additionally generate $e^+e^- \rightarrow W^+W^-$ events. As a cross check, we also generate events with HERWIG version 7.1.4 [35, 36], and find good agreement in the relevant kinematic distributions. Our study is based on truth-level information, without full detector simulation. In order for the estimate to be more realistic, we make several assumptions about the reconstruction performance, as described below, based on the performance of existing and proposed detectors.

We assume that in the reconstruction of an $e^+e^- \rightarrow Zh$ event, the final-state hadrons originating from the Higgs decay are correctly associated to the Higgs. Therefore, all particles from the Z decay are ignored at the truth level. This is especially justified, since we consider the invisible decay mode of the Z boson later on.

As discussed above, the crucial final-state hadrons for our s -tagger are kaons and charged pions, which can fake charged kaons. We make the following assumptions about their reconstruction.

Neutral kaons: Among the neutral kaons and their decays, only K_S^0 mesons decaying into two charged pions can be efficiently reconstructed. This decay is identified from the two pion tracks that form a displaced vertex. We require that the K_S^0 decay takes place at a (3-dimensional) distance of between 5 mm and 1 m from the interaction point (IP). The lower cutoff removes prompt background, and the upper one ensures that the decay occurs sufficiently deep in the detector for the pion tracks to be well reconstructed. For K_S mesons satisfying these requirements, we assume a total reconstruction efficiency of 85%. This is similar to the performance of the ATLAS detector [37].

Charged kaons: We assume that a charged pion or kaon is reconstructed with an average efficiency of 95%. In reality, an even better reconstruction efficiency is expected [38]. We further take into account the possibility that the detector has a particle identification (PID) capability, to discriminate pions from kaons. For concreteness we adopt the PID capability of the IDEA drift chamber with cluster counting, which can separate pion from kaon tracks by more than 5 standard deviations in the relevant momentum range [38]. As a parameter describing the identification of kaons candidates, we take the selection efficiency, ϵ_{K^\pm} , of the PID cut from which we obtain the misidentification probability for pions given a pion-kaon separation.

The event is divided to two hemispheres along the direction of the sphericity axis [39, 40], and each final-state

particle originating from the Higgs decay is identified with the hemisphere into which its momentum vector points. For each hemisphere we calculate J_F according to Eq. (4) with \hat{s} set to the sphericity axis. A simpler strangeness-tagging approach based on the hardest kaon of a hemisphere was employed in the DELPHI [24] and SLD [25] studies of $Z \rightarrow s\bar{s}$ decays.

Higgs decays to bottom or charm quarks are a significant background in the study of $h \rightarrow s\bar{s}$, warranting special consideration. We take advantage of the fact that bottom and charm hadrons have sufficiently large lifetimes that their decays occur visibly away from the IP. Consequently, a charged-kaon track produced in a heavy-flavor hadron decay has a non-vanishing transverse impact parameter d_0 with respect to the IP. By contrast, in a strange jet, the selected kaon candidates are produced promptly. Taking advantage of this, we further suppress the heavy-quark background by requiring a small d_0 value for all reconstructed kaon candidates with lab-frame momentum larger than 5 GeV. The momentum requirement rejects kaons for which d_0 is poorly measured.

We account for the d_0 measurement resolution by smearing the true value of d_0 for a given track with a Gaussian distribution. The Gaussian width is taken to be $\sigma_{d_0} = \sqrt{\Delta_{\text{IP}}^2 + \Delta_{d_0}^2}$, where Δ_{IP} is the uncertainty in the location of the IP, and Δ_{d_0} is the uncertainty in the location of the track. We approximate the collider-dependent [41, 42] Δ_{IP} to be 5 μm and parameterize Δ_{d_0} as a function of the kaon track momentum p and polar angle θ in the laboratory frame [43],

$$\Delta_{d_0} = \sqrt{(5 \mu\text{m})^2 + \left(\frac{10 \text{ GeV}}{p \sin^{3/2} \theta} \mu\text{m}\right)^2}. \quad (5)$$

Heavy-flavor background can be further reduced by vetoing a kaon candidate if it is part of a jet that contains additional large- d_0 tracks or a multitrack vertex that is displaced from the IP in a manner consistent with charm or bottom decay. Algorithms relying on such signatures are regularly used to select heavy-flavor jets (see, *e.g.*, Ref. [44]). Implementing these algorithms as a heavy-flavor veto involves experimental aspects that are beyond the scope of our analysis. In particular, we note that the large- J_F requirement tends to select bottom and charm hadrons that undergo few-body decays, necessitating careful study of the veto performance as a function of J_F rather than relying on studies reported in the literature for generic decays. Further improvements to background rejection can be achieved by using jet-shape variables. Since we do not implement these additional algorithms, our results on the ability of the s -tagger to reject heavy-flavor jets can be taken as conservative.

For an assessment of the general performance of the s -tagger we plot in Fig. 1 the lowest achievable s -tagger efficiency for different background channels vs. given efficiencies of the signal channel. Here, $h \rightarrow jj$ background refers to dijet Higgs decays given SM branching ratios, Non- jj background is a combination of all other back-

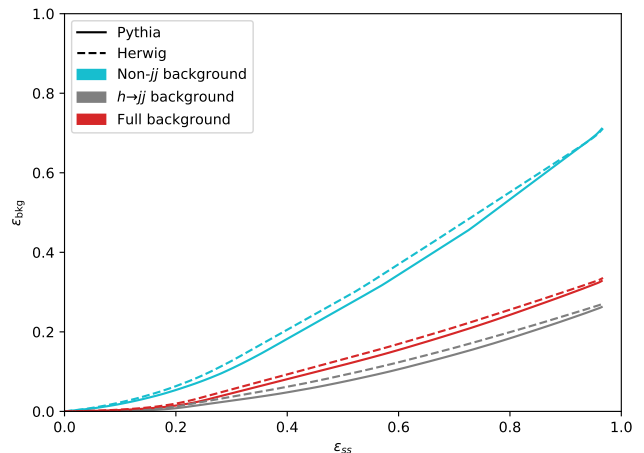


FIG. 1. Lowest possible background efficiency for specific background processes vs. given signal efficiency of the s -tagger.

ground processes as detailed below, and Full background refers to the combination of the two background classes with their relative contribution as given in Ref. [45].

We study only the signal process $e^+e^- \rightarrow Zh$ with $Z \rightarrow \nu\bar{\nu}$, which has been shown to yield the highest sensitivity to $h \rightarrow jj$ [45–48]. For an estimation of the background from non- $h \rightarrow jj$ events—events without a Higgs, events where the Higgs does not decay into two gluons or a quark–anti-quark pair, or events where the Higgs is not produced in association with two neutrinos—we rely on previous studies [45, 46]. Ref. [46] provides a conservative estimate for the achievable signal to background ratio, as it uses a too small Higgs mass of 120 GeV, thus underestimating the performance of its cut on the invariant dijet mass, m_{jj} of the Higgs candidate. Moreover, the results were obtained using a cut-and-count technique, whereas a much better signal-background separation could be obtained by using modern multivariate methods. Ref. [45] provides an estimate of the performance improvement that can be expected by using a boosted decision tree (BDT). While Refs. [46] and [45] differ significantly in their methods and in the levels of background suppression achieved, what is important for the current analysis is that they report similar flavor compositions for the non- $h \rightarrow jj$ background. Moreover, Ref. [45] reports separately selection efficiencies for different $h \rightarrow jj$ decay modes, showing that their $h \rightarrow jj$ selection efficiency is independent of the Higgs decay mode.

Refs. [45, 46] used a modular approach, in which they first applied cuts to separate $h \rightarrow jj$ from all non- $h \rightarrow jj$ background events, and then applied a flavor tag on the selected signal-rich sample to select the desired final-state flavor. We refer to these two sets of cuts as *preselection* and *flavor cuts*, respectively, and adopt the same modular approach. In the following we take the backgrounds reported in Ref. [46] and obtain the efficiency of the flavor

cuts applied within the s -tagger as follows.

The main non- $h \rightarrow jj$ background is $e^+e^- \rightarrow W^+W^-$, where one W decays leptonically, thus generating missing energy, and the other W decays hadronically. These events account for 67% of the non- $h \rightarrow jj$ background after the preselection cuts. We obtain the s -tagger efficiency for this background from the simulated $e^+e^- \rightarrow W^+W^-$ sample, taking the hadronically decaying W to fake the $h \rightarrow jj$ decay.

The remaining non- $h \rightarrow jj$ background is from the $e^+e^- \rightarrow \nu\bar{\nu}q\bar{q}$ and $e^+e^- \rightarrow q\bar{q}$ processes. In order to obtain the relative flavor composition of the quark pairs faking the Higgs boson in these processes, we generate them using MADGRAPH5 version 2.6.5 [49]. We find that the $u\bar{u}$ and $c\bar{c}$ Higgs candidates from these backgrounds account for 22% each, and the $d\bar{d}$, $s\bar{s}$, and $b\bar{b}$ Higgs candidates make up 19% each. Since here the faked Higgs has the same partonic final state as the Higgs in the generated $e^+e^- \rightarrow Zh$ samples, we take the s -tagger efficiency for these background processes from the Zh samples, accounting for the different relative contributions of the quark flavors.

Our results are summarized in Fig. 2 in terms of the number of non- $h \rightarrow jj$ events ($N_{\text{non-}jj}$) vs. the number of $h \rightarrow jj$ events (N_{jj}), obtained *after* the preselection but *before* the flavor cuts. To be precise,

$$N_{jj} = \mathcal{L} \sigma_h \mathcal{B}(h \rightarrow jj) \epsilon_{jj}, \quad (6)$$

where \mathcal{L} is the integrated luminosity, σ_h is the production cross section for $e^+e^- \rightarrow \nu\bar{\nu}h$ via both Zh and WW -fusion, $\mathcal{B}(h \rightarrow jj)$ is the total branching fraction for $h \rightarrow jj$ processes, and ϵ_{jj} is the efficiency for such an event to pass the preselection criteria. Similarly, the number of non- $h \rightarrow jj$ events after preselection is

$$N_{\text{non-}jj} = \mathcal{L} \sum_{i \in \text{non-}jj} \sigma_i \epsilon_i, \quad (7)$$

where the sum is over all the non- $h \rightarrow jj$ processes, σ_i is the cross section for the process, including relevant branching fractions, and ϵ_i is the efficiency for events of the process to pass the preselection criteria. Fig. 2 shows diagonal dashed and dotted lines of constant $N_{jj}/N_{\text{non-}jj}$, with the values of this ratio being those obtained using the cut-and-count [46] and BDT [45] techniques, respectively. On these lines, we show the points corresponding to integrated luminosities of 0.25, 5, and 20 ab^{-1} .

For a given value of N_{jj} , we determine the number of $h \rightarrow jj$ background events for the dominant Higgs decays $h \rightarrow b\bar{b}$, $h \rightarrow c\bar{c}$, and $h \rightarrow g\bar{g}$ given the SM Higgs branching fractions [50]. We also determine the number of $h \rightarrow s\bar{s}$ signal events, taking $\mathcal{B}(h \rightarrow s\bar{s}) = \mathcal{B}(h \rightarrow c\bar{c}) (m_s/m_c)^2 \approx 2.3 \times 10^{-4}$, where we evaluate the charm and strange quark masses at the Higgs mass scale using RUNDEC version 3.0 [51]. Given this composition of the $h \rightarrow jj$ events and that of the non- $h \rightarrow jj$ events, we iterate over points in the plane of Fig. 2 and evaluate the

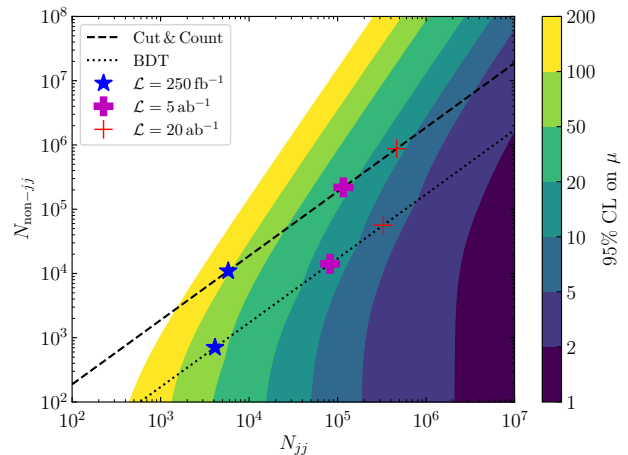


FIG. 2. The plot shows on the x -axis the number of $h \rightarrow jj$ events and on the y -axis the number of non- $h \rightarrow jj$ events, both after the preselection but before the flavor cuts. For details see text around Eqs. (6) and (7). The dashed and dotted lines show the constant ratio of $h \rightarrow jj$ to non- $h \rightarrow jj$ events obtained in a cut-and-count [46] and BDT analysis [45], respectively. Integrated luminosities for several collider benchmarks. The colored contours show the best limit on the signal strength μ_{ss} obtained after applying the s -tagger with optimized cuts and PID parameter.

number of signal and background events for varying $\epsilon_{K\pm}$ and cuts on d_0 , and J_F . We then select the cuts that yield the strongest upper limit on the signal strength μ_{ss} at 95% confidence level, and present the upper limits as contours in Fig. 2.

For small values of the ratio $N_{jj}/N_{\text{non-}jj}$ —around and above the cut-and-count line—very loose flavor cuts yield the strongest, yet weak limits on μ_{ss} . For the larger values of $N_{jj}/N_{\text{non-}jj}$ obtained by the BDT analysis [45], $h \rightarrow jj$ becomes the dominant background, so that tighter flavor cuts significantly increase the sensitivity to the $h \rightarrow s\bar{s}$ decay when the luminosity is sufficiently large. For the 5 ab^{-1} benchmark on the BDT line the best results are still obtained for a working point with loose cuts yielding a signal efficiency of $\epsilon_{ss} \approx 96\%$ and correspondingly background efficiencies of $\epsilon_{\text{bkg}}^{h \rightarrow jj} \approx 26\%$ and $\epsilon_{\text{bkg}}^{\text{non-}jj} \approx 70\%$. For the 20 ab^{-1} benchmark, a tight flavor tag is preferred for the PYTHIA set, yielding $\epsilon_{ss} \approx 14\%$, $\epsilon_{\text{bkg}}^{h \rightarrow jj} < 1\%$, and $\epsilon_{\text{bkg}}^{\text{non-}jj} \approx 3\%$. With these points we obtain an upper limit on the signal strength of $\mu_{ss} \lesssim 14$ and $\lesssim 7$ for integrated luminosities of 5 and 20 ab^{-1} , respectively. The limit is weakened to $\mu_{ss} \lesssim 60$ for an integrated luminosity of 250 fb^{-1} .

The limits in Fig. 2 do not include systematic uncertainties. However, given the small number of signal events, the experimental analysis will be statistics limited. For an estimate of the systematic uncertainty on our predictions we compare the values of μ_{ss} obtained with the data sets generated with PYTHIA and HERWIG, re-

spectively, and find them to differ by less than 2% for the three luminosity benchmarks indicated on the BDT and cut-and-count lines. Only when the non- $h \rightarrow jj$ background is reduced to less than about 10% of the total background does the difference increase to 15-20%. By studying the s -tagger performance with the large sample collected by a future collider, particularly in Z decays and 3-jet events, this uncertainty will be greatly reduced.

We have shown that even with a simple tagging algorithm a very large improvement could be obtained at a high-luminosity lepton collider, making it sensitive to the strange Yukawa coupling at the level of several times the SM prediction. This is to be compared to the es-

timated limit obtainable at the HL-LHC ranging from $\mu_{ss}^{\text{HL-LHC}} \lesssim 200$ from a global fit to $\mu_{ss}^{\text{HL-LHC}} \lesssim 10^7$ from the exclusive decay [52].

ACKNOWLEDGMENTS

We thank Marumi Kado and Fabio Maltoni for useful discussions. The work of GP is supported by grants from the BSF, ERC, ISF, the Minerva Foundation, and the Segre Research Award. AS is supported by grants from the BSF, GIF, and ISF, and the European Unions Horizon 2020 Marie Skłodowska-Curie programme.

-
- [1] G. F. Giudice and O. Lebedev, *Phys. Lett.* **B665**, 79 (2008), [arXiv:0804.1753 \[hep-ph\]](#).
- [2] C. Delaunay, T. Golling, G. Perez, and Y. Soreq, *Phys. Rev.* **D89**, 033014 (2014), [arXiv:1310.7029 \[hep-ph\]](#).
- [3] A. L. Kagan, G. Perez, F. Petriello, Y. Soreq, S. Stoynev, and J. Zupan, *Phys. Rev. Lett.* **114**, 101802 (2015), [arXiv:1406.1722 \[hep-ph\]](#).
- [4] A. Dery, A. Efrati, Y. Nir, Y. Soreq, and V. Susi, *Phys. Rev.* **D90**, 115022 (2014), [arXiv:1408.1371 \[hep-ph\]](#).
- [5] M. Bauer, M. Carena, and K. Gemmler, *JHEP* **11**, 016 (2015), [arXiv:1506.01719 \[hep-ph\]](#).
- [6] D. Ghosh, R. S. Gupta, and G. Perez, *Phys. Lett.* **B755**, 504 (2016), [arXiv:1508.01501 \[hep-ph\]](#).
- [7] M. Aaboud *et al.* (ATLAS), *Phys. Lett.* **B786**, 59 (2018), [arXiv:1808.08238 \[hep-ex\]](#).
- [8] M. Aaboud *et al.* (ATLAS), *Phys. Lett.* **B784**, 173 (2018), [arXiv:1806.00425 \[hep-ex\]](#).
- [9] M. Aaboud *et al.* (ATLAS), *Phys. Rev.* **D99**, 072001 (2019), [arXiv:1811.08856 \[hep-ex\]](#).
- [10] A. M. Sirunyan *et al.* (CMS), *Eur. Phys. J.* **C79**, 421 (2019), [arXiv:1809.10733 \[hep-ex\]](#).
- [11] M. Aaboud *et al.* (ATLAS), *Phys. Rev. Lett.* **119**, 051802 (2017), [arXiv:1705.04582 \[hep-ex\]](#).
- [12] V. Khachatryan *et al.* (CMS), *Phys. Lett.* **B744**, 184 (2015), [arXiv:1410.6679 \[hep-ex\]](#).
- [13] G. Perez, Y. Soreq, E. Stamou, and K. Tobioka, *Phys. Rev.* **D92**, 033016 (2015), [arXiv:1503.00290 \[hep-ph\]](#).
- [14] M. Aaboud *et al.* (ATLAS), *JHEP* **07**, 127 (2018), [arXiv:1712.02758 \[hep-ex\]](#).
- [15] G. T. Bodwin, F. Petriello, S. Stoynev, and M. Velasco, *Phys. Rev.* **D88**, 053003 (2013), [arXiv:1306.5770 \[hep-ph\]](#).
- [16] M. Greco, T. Han, and Z. Liu, *Phys. Lett.* **B763**, 409 (2016), [arXiv:1607.03210 \[hep-ph\]](#).
- [17] I. Brivio, F. Goertz, and G. Isidori, *Phys. Rev. Lett.* **115**, 211801 (2015), [arXiv:1507.02916 \[hep-ph\]](#).
- [18] F. Bishara, U. Haisch, P. F. Monni, and E. Re, *Phys. Rev. Lett.* **118**, 121801 (2017), [arXiv:1606.09253 \[hep-ph\]](#).
- [19] Y. Soreq, H. X. Zhu, and J. Zupan, *JHEP* **12**, 045 (2016), [arXiv:1606.09621 \[hep-ph\]](#).
- [20] F. Yu, *JHEP* **02**, 083 (2017), [arXiv:1609.06592 \[hep-ph\]](#).
- [21] J. Gao, *JHEP* **01**, 038 (2018), [arXiv:1608.01746 \[hep-ph\]](#).
- [22] G. Perez, Y. Soreq, E. Stamou, and K. Tobioka, *Phys. Rev.* **D93**, 013001 (2016), [arXiv:1505.06689 \[hep-ph\]](#).
- [23] J. F. Kamenik, G. Perez, M. Schlaffer, and A. Weiler, *Eur. Phys. J.* **C77**, 126 (2017), [arXiv:1607.06440 \[hep-ph\]](#).
- [24] P. Abreu *et al.* (DELPHI), *Eur. Phys. J.* **C14**, 613 (2000).
- [25] M. Kalelkar *et al.* (SLD), *Quantum chromodynamics. Proceedings, 8th Conference, 5th Euroconference, QCD 2000, Montpellier, France, July 6-13, 2000*, *Nucl. Phys. Proc. Suppl.* **96**, 31 (2001), [31(2000)], [arXiv:hep-ex/0008032 \[hep-ex\]](#).
- [26] T. Barklow, J. Brau, K. Fujii, J. Gao, J. List, N. Walker, and K. Yokoya, (2015), [arXiv:1506.07830 \[hep-ex\]](#).
- [27] M. Benedikt *et al.*, in *Proceedings, 6th International Particle Accelerator Conference (IPAC 2015): Richmond, Virginia, USA, May 3-8, 2015* (2015) p. TUPTY061.
- [28] CEPC Study Group, (2018), [arXiv:1809.00285 \[physics.acc-ph\]](#).
- [29] X. Mo, G. Li, M.-Q. Ruan, and X.-C. Lou, *Chin. Phys.* **C40**, 033001 (2016), [arXiv:1505.01008 \[hep-ex\]](#).
- [30] M. Thomson, *Eur. Phys. J.* **C76**, 72 (2016), [arXiv:1509.02853 \[hep-ex\]](#).
- [31] A. Banfi, G. P. Salam, and G. Zanderighi, *Eur. Phys. J.* **C47**, 113 (2006), [arXiv:hep-ph/0601139 \[hep-ph\]](#).
- [32] P. Ilten, N. L. Rodd, J. Thaler, and M. Williams, *Phys. Rev.* **D96**, 054019 (2017), [arXiv:1702.02947 \[hep-ph\]](#).
- [33] T. Sjöstrand, S. Mrenna, and P. Z. Skands, *JHEP* **05**, 026 (2006), [arXiv:hep-ph/0603175 \[hep-ph\]](#).
- [34] T. Sjöstrand, S. Ask, J. R. Christiansen, R. Corke, N. Desai, P. Ilten, S. Mrenna, S. Prestel, C. O. Rasmussen, and P. Z. Skands, *Comput. Phys. Commun.* **191**, 159 (2015), [arXiv:1410.3012 \[hep-ph\]](#).
- [35] M. Bahr *et al.*, *Eur. Phys. J.* **C58**, 639 (2008), [arXiv:0803.0883 \[hep-ph\]](#).
- [36] J. Bellm *et al.*, *Eur. Phys. J.* **C76**, 196 (2016), [arXiv:1512.01178 \[hep-ph\]](#).
- [37] ATLAS Collaboration, *Performance of the reconstruction of large impact parameter tracks in the ATLAS inner detector*, Tech. Rep. ATL-PHYS-PUB-2017-014 (CERN, Geneva, 2017).
- [38] A. Abada *et al.* (FCC), *Eur. Phys. J. ST* **228**, 261 (2019).
- [39] G. Parisi, *Phys. Lett.* **74B**, 65 (1978).
- [40] J. F. Donoghue, F. E. Low, and S.-Y. Pi, *Phys. Rev.* **D20**, 2759 (1979).
- [41] B. Barish and J. E. Brau, *Int. J. Mod. Phys.* **A28**, 1330039 (2013), [arXiv:1311.3397 \[physics.acc-ph\]](#).
- [42] M. Boscolo and M. K. Sullivan, *ICFA Beam Dyn.*

- Newslett. **72**, 70 (2017).
- [43] H. Abramowicz *et al.*, (2013), [arXiv:1306.6329 \[physics.ins-det\]](#).
- [44] M. Aaboud *et al.* (ATLAS), *JHEP* **08**, 089 (2018), [arXiv:1805.01845 \[hep-ex\]](#).
- [45] Y. Bai, “ $H \rightarrow bb/cc/gg$ Branch Ratio Measurement in CEPC,” 3rd CEPC Physics Software Meeting, <http://indico.ihep.ac.cn/event/6495/session/1/contribution/6/material/slides/0.pdf> (2016).
- [46] H. Ono and A. Miyamoto, *Eur. Phys. J.* **C73**, 2343 (2013), [arXiv:1207.0300 \[hep-ex\]](#).
- [47] H. Abramowicz *et al.*, *Eur. Phys. J.* **C77**, 475 (2017), [arXiv:1608.07538 \[hep-ex\]](#).
- [48] M. Dong *et al.* (CEPC Study Group), (2018), [arXiv:1811.10545 \[hep-ex\]](#).
- [49] J. Alwall, R. Frederix, S. Frixione, V. Hirschi, F. Maltoni, O. Mattelaer, H. S. Shao, T. Stelzer, P. Torrielli, and M. Zaro, *JHEP* **07**, 079 (2014), [arXiv:1405.0301 \[hep-ph\]](#).
- [50] D. de Florian *et al.* (LHC Higgs Cross Section Working Group), (2016), [10.23731/CYRM-2017-002, arXiv:1610.07922 \[hep-ph\]](#).
- [51] F. Herren and M. Steinhauser, *Comput. Phys. Commun.* **224**, 333 (2018), [arXiv:1703.03751 \[hep-ph\]](#).
- [52] M. Cepeda *et al.* (HL/HE WG2 group), (2019), [arXiv:1902.00134 \[hep-ph\]](#).